Biomedicine & Pharmacotherapy 160 (2023) 114315

Contents lists available at ScienceDirect

Biomedicine & Pharmacotherapy

journal homepage: www.elsevier.com/locate/biopha

Isoalantolactone protects against ethanol-induced gastric ulcer via alleviating inflammation through regulation of PI3K-Akt signaling pathway and Th17 cell differentiation

Chaoyi Zhou [a,b], Jing Chen [c], Kechun Liu [b], Kannan Maharajan [b], Yun Zhang [b], Linhua Hou [a,b], Jianheng Li [a,*], Ma Mi [c,*], Qing Xia [b,*]

[a] School of Pharmacy, Hebei University, Baoding 071002, China
[b] Biology Institute, Qilu University of Technology (Shandong Academy of Sciences), Jinan 250103, China
[c] Tibetan traditional medicine college, Lhasa 850000, China

ARTICLE INFO

Keywords:
Isoalantolactone
Gastric ulcer
Anti-inflammatory effect
Network pharmacology
Zebrafish

ABSTRACT

Gastric ulcer (GU) is one of the most prevalent digestive system diseases in humans, and it has been linked to inflammation. Previous studies have demonstrated the anti-inflammatory potential of isoalantolactone (IAL), a sesquiterpene lactone isolated from Radix Inulae. However, the pharmacological effects of IAL on GU and its mechanism of action are still unclear. Hence, the present study is aimed to investigate the anti-inflammatory potential of IAL on GU. Firstly, we assessed the effect of IAL on ethanol-induced injury of human gastric epithelial cells and the levels of inflammatory cytokines in cell culture supernatants. Then, the anti-inflammatory effects of IAL were confirmed in vivo using zebrafish inflammation models. Furthermore, the mechanism of IAL against GU was preliminarily discussed through network pharmacology and molecular docking studies. Quantitative real-time PCR assays were also used to confirm the mechanism of IAL action. ALB, EGFR, SRC, HSP90AA1, and CASP3 were found for the first time as the key targets of the IAL anti-GU. PI3K-Akt signaling pathway and Th17 cell differentiation were identified to play a crucial role in the anti-GU effects of IAL. In conclusion, we found that IAL has anti-inflammatory effects both in vitro and in vivo, and showed potential protective effects against ethanol-induced GU.

1. Introduction

Gastric ulcer (GU) is one of the most common digestive system diseases in humans, with an incidence rate of 2.4% in the western population and 6.1% in the Chinese population [1]. Alcohol is one of the most common causes of gastric injury [2]. Ethanol damages the gastric mucosa by affecting the balance of the gastric mucosal barrier, promoting the infiltration of inflammatory cells and the release of inflammatory factors [3]. As we know, gastric mucosal epithelial cell injury is a critical factor in the formation of GU and a common feature of GU. Many drugs such as proton pump inhibitors have been used clinically to alleviate GU. However, the long-term use of omeprazole and other chemically synthesized drugs to treat GU has serious side effects and a high recurrence rate [4]. Therefore, there is a need for a safe and effective natural active substance to prevent and treat ethanol-induced gastric injury. At present, the use of natural chemicals such as terpenoids, flavonoids, polysaccharides from plant resources as medicines or food supplements has received extensive attention among researchers [5].

Our previous work supported that Sanwei Ganlu San (SWG, a kind of Tibetan herbal formula) had a good anti-GU effect. Radix Inulae (dried root of *Inula helenium* L. or *I. racemosa* Hook. F.) is one of the ingredients of SWG. Radix Inulae is traditionally used to treat epigastric pain, bloating, vomiting, and diarrhea [6]. We further found that IAL was a main chemical component of SWG (the relative content is 3.26%), and it is also a main component migrating to blood. IAL is also one of the main sesquiterpene lactones in Radix Inulae, with anti-inflammatory, antibacterial, anti-lipogenic, and anti-tumor effects [7]. Studies have shown that IAL alleviates ovalbumin-induced asthmatic inflammation [8]. In addition, IAL also inhibits LPS-induced inflammation and alleviates acute lung injury [9]. IAL has been reported to improve the survival of mice with LPS-induced sepsis and exhibits anti-inflammatory activity [10]. However, the pharmacological effects of IAL on GU and its

* Corresponding authors.
E-mail addresses: lijianheng@hbu.cn (J. Li), mm2626@163.com (M. Mi), sdxq1021@163.com (Q. Xia).

https://doi.org/10.1016/j.biopha.2023.114315
Received 26 November 2022; Received in revised form 10 January 2023; Accepted 26 January 2023
Available online 28 January 2023

mechanism of action are still unclear.

The use of zebrafish models for drug screening has unique advantages because of its complete vertebrate organ system, which can exhibit diverse biological processes [11]. The zebrafish genome has been fully sequenced and has a high degree of similarity to the human genome [12]. In addition, zebrafish display inflammatory cells and immune responses similar to humans, while the transparency of zebrafish larvae enables visualization of inflammatory cell migration. The zebrafish inflammation model has been well-established, which is mainly induced by $CuSO_4$, tail-cutting, and lipopolysaccharide (LPS) [13].

Network pharmacology, as a powerful tool to predict complex relationships among drugs, targets, and diseases, has been successfully applied to reveal the mechanisms of action of traditional Chinese medicine (TCM) components and diseases [14]. Molecular docking studies enable the binding of small molecule drugs with target proteins in space and clarify the binding activity between drugs and targets. Therefore, the combination of network pharmacology and molecular docking further reveals the mechanism of action of drugs. Cells, zebrafish, network pharmacology, and molecular docking are all good models and methods to obtain valuable results before animal experiments. These models and methods follow the "3 R" roles.

In the present study, we evaluated the effects of IAL on ethanol-induced injury in human gastric epithelial (GES-1) cells and examined the levels of inflammatory cytokines in cell culture supernatants. The anti-inflammatory effects of IAL were studied in vivo using zebrafish inflammation models. Further, the mechanism of IAL action against GU was preliminarily discussed through network pharmacology, molecular docking studies, and quantitative real-time PCR validation.

2. Materials and methods

2.1. Materials and reagents

Isoalantolactone (CAS: 470–17–7, purity≥98%) was purchased from Chengdu DeSiTe Biological Technology Co., Ltd. (Chengdu, Sichuan, China). Zebrafish culture water was prepared with 5 mM NaCl , 0.17 mM KCl , 0.33 mM $CaCl_2$, 0.33 mM $MgSO_4{\cdot}7\ H_2O$. Tricaine and lipopolysaccharides (LPS) were purchased from Sigma-Aldrich (St. Louis, USA). Ethanol was procured from Tianjin Fuyu Fine Chemical Co., Ltd. (Tianjin, China). Ibuprofen and omeprazole were obtained from Shanghai Yuanye Biotechnology Co., Ltd. (Shanghai, China). $CuSO_4{\cdot}5\ H_2O$ and methylene blue were purchased from Sinopharm Chemical Reagent Co., Ltd. (Shanghai, China). Fetal bovine serum (FBS) was obtained from AusGeneX (Gold Coast, Australia). RPMI1640 cell culture medium, penicillin/streptomycin solution (100 ×), and cell counting kit-8 (CCK-8) were procured from GENVIEW® (Jinan, Shandong, China). The tumor necrosis factor-α (TNF-α), interleukin (IL)− 1β, interleukin (IL)− 10, interferons-γ (IFN-γ), transforming Growth Factor Beta 1 (TGF-β1), and vascular endothelial growth factor A (VEGFA) ELISA kits were purchased from ABclonal Biotechnology Co., Ltd. (Wuhan, Hubei, China). Reactive oxygen species (ROS) assay kit was obtained from Solarbio (Beijing, China).

The details of the instruments utilized in this study were listed below, SERIES 8000 WJ CO_2 Incubator (Thermo Fisher Scientific, Waltham, USA); BMG LABTECH Multi-function Microplate Reader (BIO-GENE, Guangzhou, China); ZXSD-B1270 biochemical incubator (Shanghai Zhicheng Analytical Instrument Manufacturing Co., Ltd., Shanghai, China); SZX16 Fluorescence Microscope and DP2-BSW Image Acquisition System (Olympus, Tokyo, Japan); Stereo Microscope Axio Zoom. V16 (Zeiss, Oberkochen, Germany); Zebrafish breeding equipment (Beijing Aisheng Technology Company, Beijing, China); HPG-280BX light incubator (Harbin Donglian Electronic Technology Development Co., Ltd., Harbin, China) and Real-time fluorescence quantitative PCR instrument (Light Cycler® Instrument, Roche, Switzerland).

2.2. Cell culture

GES-1 cells (Zhejiang Meisen Cell Technology Co., Ltd., Zhejiang, China) were incubated in RPMI1640 cell culture medium supplemented with 10% FBS and 1% penicillin/streptomycin solution. Then, the culture was maintained at 37 °C in a constant temperature incubator with 5% CO_2.

2.3. Gastroprotective effects of IAL in vitro

To evaluate the gastroprotective effects of IAL on the ethanol-induced cell injury model, GES-1 cells were treated with 7% (vol/vol) ethanol for 3 h to establish a gastric injury model. Briefly, 5×10^3 cells/well were seeded in a 96-well plate and incubated for 24 h. Then, the culture was divided into different groups such as the control group (medium), model group (medium), positive control group (20 μg/ml omeprazole), and treatment groups with different concentrations of IAL (1.25, 2.5, and 5 μM) and further cultured for 24 h. Except for the control group, cells in all other groups were treated with 7% (vol/vol)) ethanol for 3 h. Later, the cell viability was assessed using the CCK-8 kit following manufacturer instructions. The optical density (OD) value was measured on a microplate reader at 450 nm. The cell viability was calculated according to Eq. (1), where A_s, A_b, and A_c represent the absorbance difference of experimental, blank, and control groups, respectively.

$$Cell\ viability(\%) = \frac{A_s - A_b}{A_c - A_b} \times 100\% \quad (1)$$

2.4. Determination of inflammatory cytokines

The inflammatory cytokines TNF-α, IL-1β, IFN-γ, IL-10, TGF-β1, and VEGFA level in GES-1 supernatant were determined using the ELISA kits. The OD value was measured on a microplate reader at 450 nm. All tests were carried out following the kit instructions.

2.5. Zebrafish preparation

Transgenic zebrafish with green fluorescent labeled immune cells (Tg: lyz-EGFP) and wild-type AB zebrafish were fed twice a day and housed at 28 ℃ under 14 h light/10 h dark conditions. The day before mating, male and female zebrafish were placed in spawning tanks in a 2:2 ratio. Zebrafish embryos were obtained from 10:00–11:00 a.m. on the day of mating and washed 3 times with water. After washing, the embryos were transferred to zebrafish culture water containing 0.1% methylene blue and incubated at 28 ℃ under light control. At three days post-fertilization (dpf), healthy larvae were selected under the microscope for further experiments. All experiments were carried out in compliance with the standard ethical guidelines and under the control of the Biology Institute, Qilu University of Technology Animal Ethics Committee.

2.6. Anti-inflammatory effects of IAL

2.6.1. $CuSO_4$-induced inflammation model

Healthy zebrafish larvae (3 dpf) were transferred into 24-well culture plates (10 larvae per well) and grouped as control group (zebrafish culture water), model group, positive control group (10 μM ibuprofen solution), and experimental groups of IAL with different doses (1.25, 2.5, and 5 μM). After incubation for 24 h, except for the control group, the medium of all other groups was replaced with 40 μM $CuSO_4$ solution for 1 h. Finally, the zebrafish larvae in each group were anesthetized with tricaine (0.3%) for 1 min and fixed in the lateral position on a glass slide. The immune cells as an inflammatory response were observed under the fluorescence microscope, and the number of immune cells that migrated to the lateral line (cloaca to tail) was counted in the zebrafish

larvae.

2.6.2. Tail cutting-induced inflammation model

Healthy zebrafish larvae (3 dpf) were transferred into 24-well culture plates, with 10 larvae per well. The experimental group settings were the same as in section "2.6.1". Except for the control group, the zebrafish larvae in other groups were first anesthetized with tricaine for 1 min, followed by the tail transection with a blade, and then recovered with zebrafish culture water. After 6 h of incubation, zebrafish larvae were placed on a glass slide and fluorescent immune cells were visualized under the microscope. Image-Pro Plus 5.1 software was used to analyze the integral optical density (IOD) value of immune cells migrating to the mechanically damaged area (cross-section of the tail).

2.6.3. LPS-induced inflammation model

For the LPS-induced inflammation model, 10 healthy zebrafish larvae (3 dpf) were transferred into each well in a 24-well culture plate. The experimental groups were the same as mentioned in section "2.6.1". LPS (100 μg/ml) was administered simultaneously with different concentrations of IAL for three days. On the fourth day, the behavior of green fluorescently labeled immune cells was observed under a microscope. IOD values of zebrafish systemic immune cells were analyzed by Image-Pro Plus 5.1 software.

2.7. ROS detection

To study the accumulation of intracellular ROS in the $CuSO_4$-induced inflammatory response, wild-type AB zebrafish larvae were randomly transferred to a 24-well plate (10 larvae per well) and followed the administration method in "2.6.1". Then the larvae were treated with 2',7'-dichlorodihydrofluorescein diacetate (DCFH-DA) solution (10 μM) for 1 h in the dark. After anesthesia with tricaine, zebrafish larvae were photographed under a fluorescence microscope. IOD values in individual zebrafish larvae were analyzed using Image-Pro Plus 5.1 software.

2.8. Network pharmacology analysis

2.8.1. Target prediction for IAL

The 2D structure or Canonical SMILES of IAL was obtained using the PubChem database (https://pubchem.ncbi.nlm.nih.gov/), imported into the PharmMapper database (http://www.lilab-ecust.cn/pharmmapper/) and the Swiss Target Prediction database (http://www.swisstargetprediction.ch/), to collect the targets of IAL. TCMSP database (https://tcmspw.com/) was also searched. Finally, we used the Uniprot database (http://www.uniprot.org/) to correct the gene names.

2.8.2. Target prediction for GU

With "gastric ulcer" as the keyword, the TCMSP (https://tcmspw.com/), GeneCards (https://www.genecards.org/), CTD (http://ctdbase.org/), DisGeNET (http://www.disgenet.org/home/), and TTD (http://db.idrblab.net/ttd/) databases were used to search, and the GU-related targets were collected after removing duplicates.

2.8.3. Network construction

Venn analysis was carried out on the targets of IAL and GU-related targets, and the potential targets of IAL against GU were screened. Then, we used Cytoscape v.3.9.0 analysis software to construct the "IAL-targets-GU" visualization network diagram.

2.8.4. Topological analysis

The potential targets of IAL against GU were imported into the String online analysis platform (https://string-db.org/). "Multiple proteins" and "Homo sapiens" were selected for analysis. A "protein-protein interaction" (PPI) network was obtained and visualized by Cytoscape. Nodes above the median degrees were screened to be crucial targets in the network.

Table 1
Primer Sequences Listing.

Gene	Primer orientation	Nucleotide sequence
rpl13a	Forward	5'-TCTGGAGGACTGTAAGAGGTATGC-3'
	Reverse	5'-AGACGCACAATCTTGAGAGCAG − 3'
mapk10	Forward	5'-GGTGCGCCACAAAATCCTATT-3'
	Reverse	5'-TAAACTCAGGAGAGGGCGTG-3'
mapk8b	Forward	5'-TGCTGGCATCATACACAGGG-3'
	Reverse	5'-GGCCCGATAATAGCGTGTCA-3'
mapk14a	Forward	5'-GCCATGAGGCTCGTACTTACAT-3'
	Reverse	5'-ATCCGGGTCATGATATTGGGC-3'
mapk14b	Forward	5'-AGGGCCTGAGCTCTTGATGAAAAT-3'
	Reverse	5'-TGTGTCCAGAACCAGCATCTT-3'
mapk1	Forward	5'-CGCTTACGGCATGGTTTGTT-3'
	Reverse	5'-TACGTCTGGTGCTCAAACGG-3'
map2k1	Forward	5'-AAGATCAGCGAGTTGGGAGC-3'
	Reverse	5'-GAAGCCCACGATGTAGGGAG-3'
pgf	Forward	5'-CGGTGCAGTTGAGCCTTTTAC-3'
	Reverse	5'-CCCCCAAACCTCCTGAAACA-3'
egfr	Forward	5'-GCCGCAAAGTGTGTAACGG-3'
	Reverse	5'-GTCACCCCTAAATGCCACCG-3'
fgfr1	Forward	5'-TGCTCAAATCGGACGCCACA-3'
	Reverse	5'-TTAGCAGCAAACTCCACGATG-3'
rara	Forward	5'-GAGAGTGTGGATGTGAACCCT-3'
	Reverse	5'-GATGAGCTGAAGGGATGGGG-3'
rxra	Forward	5'-ACCTGAACAGAAGCAGACAGTA-3'
	Reverse	5'-GGGACCTTCATCACCCCGTT-3'
rxrb	Forward	5'-ATCAGCTCATCCCTGGGGTC-3'
	Reverse	5'-CGGTGGAGTTGATCTGTGGG-3'
tnf-α	Forward	5'-GGGCAATCAACAAGATGGAAG-3'
	Reverse	5'-GCAGCTGATGTGCAAAGACAC-3'
ifn-γ	Forward	5'-CTCGCATGCAGAATGACAGC-3'
	Reverse	5'-TCGTTTTCCTTGATCGCCCA-3'
tgf-β1	Forward	5'-GTCCGAGATGAAGCGCAGTA-3'
	Reverse	5'-TGGAGACAAAGCGAGTTCCC-3'

2.8.5. Bioinformatic annotation

Gene ontology (GO) and Kyoto Encyclopedia of Genes and Genomes (KEGG) pathway enrichment analyses were performed on the David online analysis platform (https://david.ncifcrf.gov/) to screen the GO processes and signaling pathways involved in the potential targets of IAL against GU.

2.9. Molecular docking verification of key targets

To elucidate the binding activity of IAL to its potential targets against GU, the binding ability of IAL to the top five targets in the PPI network was verified by molecular docking. The mol2 format file of IAL was downloaded from the TCMSP database (https://tcmspw.com/), and the crystal structure of the core target protein receptor was downloaded from the RCSB PDB database (https://www.rcsb.org/). Ligand small molecule and core protein structures were pre-processed using Discovery Studio 2016 software, followed by molecular docking. The docking results are given by the scoring function LibDock Score. The higher the LibDock Score, the higher the binding activity of the predicted component to the target.

2.10. Quantitative real-time PCR (qPCR)

Zebrafish larvae were first treated with 1.25, 2.5, and 5 μM IAL for 24 h, and then treated with 40 μM $CuSO_4$ for 1 h. The total RNA from each group of zebrafish larvae was extracted with FastPure Cell/Tissue Total RNA Isolation Kit V2, and reverse transcribed into cDNA with HiScript III RT SuperMix for qPCR (+gDNA wiper). Quantitative real-time PCR detection was performed according to manufacturer instructions using the SYBR Green fluorescence quantitative PCR kit, with *rpl13a* as the internal reference gene. The differences in gene expression were displayed by the $2^{-\Delta\Delta Ct}$ (Livak and Schmittgen, 2001) method. The primer sequences used in this study are shown in Table 1.

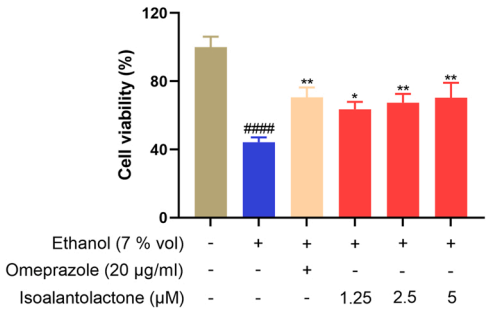

Fig. 1. Effects of different concentrations of IAL treatment on cell viability after ethanol injury. Data are expressed as mean ± SEM (n = 5). ####P < 0.0001 vs. the control group, *P < 0.05, **P < 0.01 vs. the model group.

2.11. Statistical analysis

Data were expressed as mean ± standard error of mean (SEM) from at least three independent experiments. Comparison of means among multiple groups was accomplished by one-way analysis of variance (ANOVA), with Dunnett's multiple comparisons test. P < 0.05 was considered to be statistically significant.

3. Results

3.1. Gastroprotective effects of IAL in vitro

After being treated with 7% (vol/vol) ethanol, the cell viability of GES-1 cells decreased significantly, indicating ethanol-induced GES-1 cell damage. However, 1.25, 2.5, and 5 μM IAL could significantly increase the cell viability of GES-1 cells (Fig. 1). This implied that IAL was likely to protect the cell impairment by ethanol.

3.2. Levels of inflammatory cytokines in GES-1 supernatant

Ethanol exposure could significantly increase the pro-inflammatory cytokines (TNF-α, IL-1β, IFN-γ) levels and reduced the anti-inflammatory cytokines (IL-10, TGF-β1, VEGFA) levels (Fig. 2). However, IAL could significantly reverse this phenomenon induced by ethanol.

3.3. Anti-inflammatory effects of IAL

Three zebrafish inflammation models induced by $CuSO_4$, tail-cutting, and LPS were used to confirm the anti-inflammatory effect of IAL. As shown in Fig. 3 A, a large number of immune cells migrated to the lateral line of the zebrafish larvae nerve after exposure to $CuSO_4$. However, IAL significantly inhibited the migration of immune cells induced by $CuSO_4$ (Fig. 3B). In tail cutting-induced mechanical injury, inflammatory cells accumulated significantly at the injured site (Fig. 3 C). While, IAL significantly inhibited the recruitment of immune cells in a dose-dependent manner (Fig. 3D). LPS can induce a systemic inflammatory response in zebrafish (Fig. 3E). Compared with the model group, IAL could significantly reduce the IOD value of zebrafish larvae immune cells (Fig. 3 F). Altogether, these results confirmed that IAL had significant anti-inflammatory effects.

3.4. ROS detection

The alleviative effect of IAL on inflammation was studied in zebrafish larvae by measuring ROS. As shown in Fig. 4, the model group exposed to $CuSO_4$ had higher IOD values compared to the control group. Therefore, the addition of $CuSO_4$ could lead to the generation of ROS in zebrafish cells. However, after IAL treatment, a dose-dependent reduction in ROS accumulation was observed in zebrafish cells.

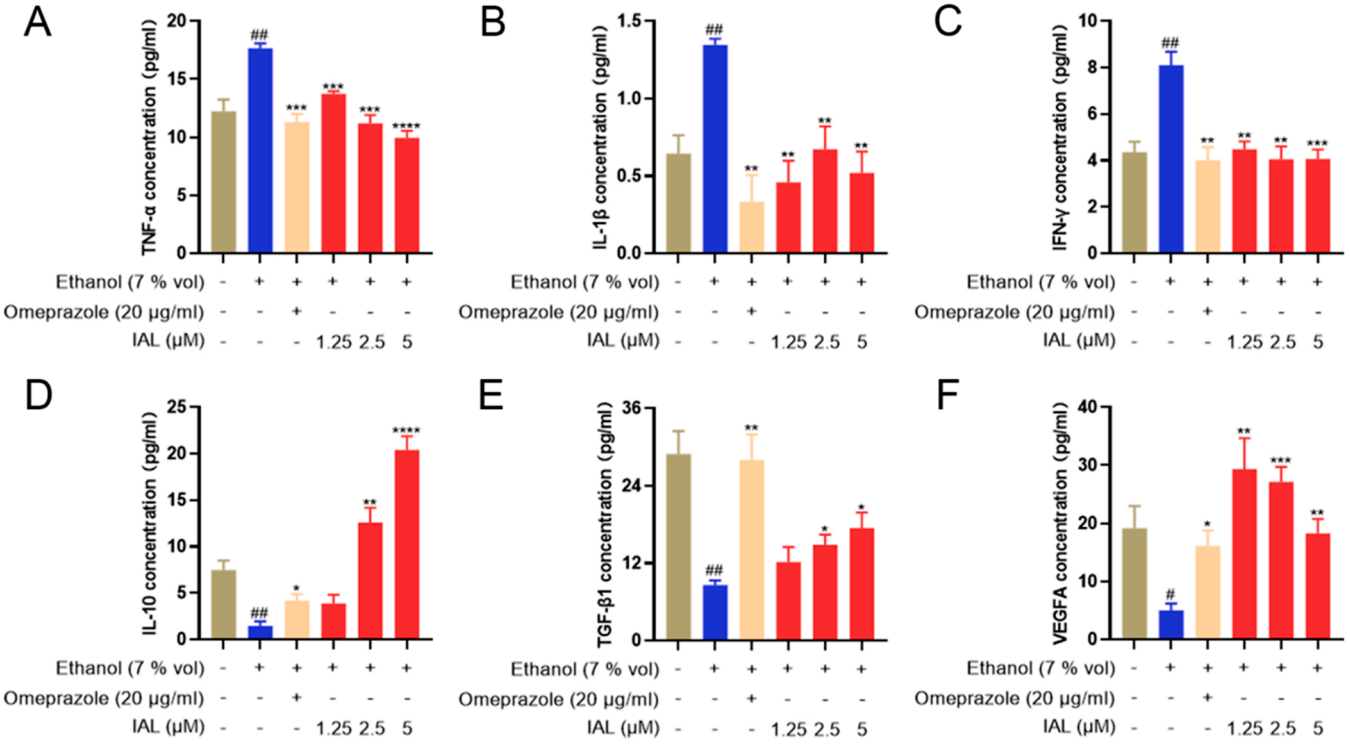

Fig. 2. Effect of IAL on the levels of pro-inflammatory cytokines (TNF-α, IL-1β, and IFN-γ) and anti-inflammatory cytokines (IL-10, TGF-β1, and VEGFA), in ethanol-stimulated GES-1 supernatant. Data are expressed as mean ± SEM (n = 5). #P < 0.05, ##P < 0.01 vs. the control group, *P < 0.05, **P < 0.01, ***P < 0.001, ****P < 0.0001 vs. the model group.

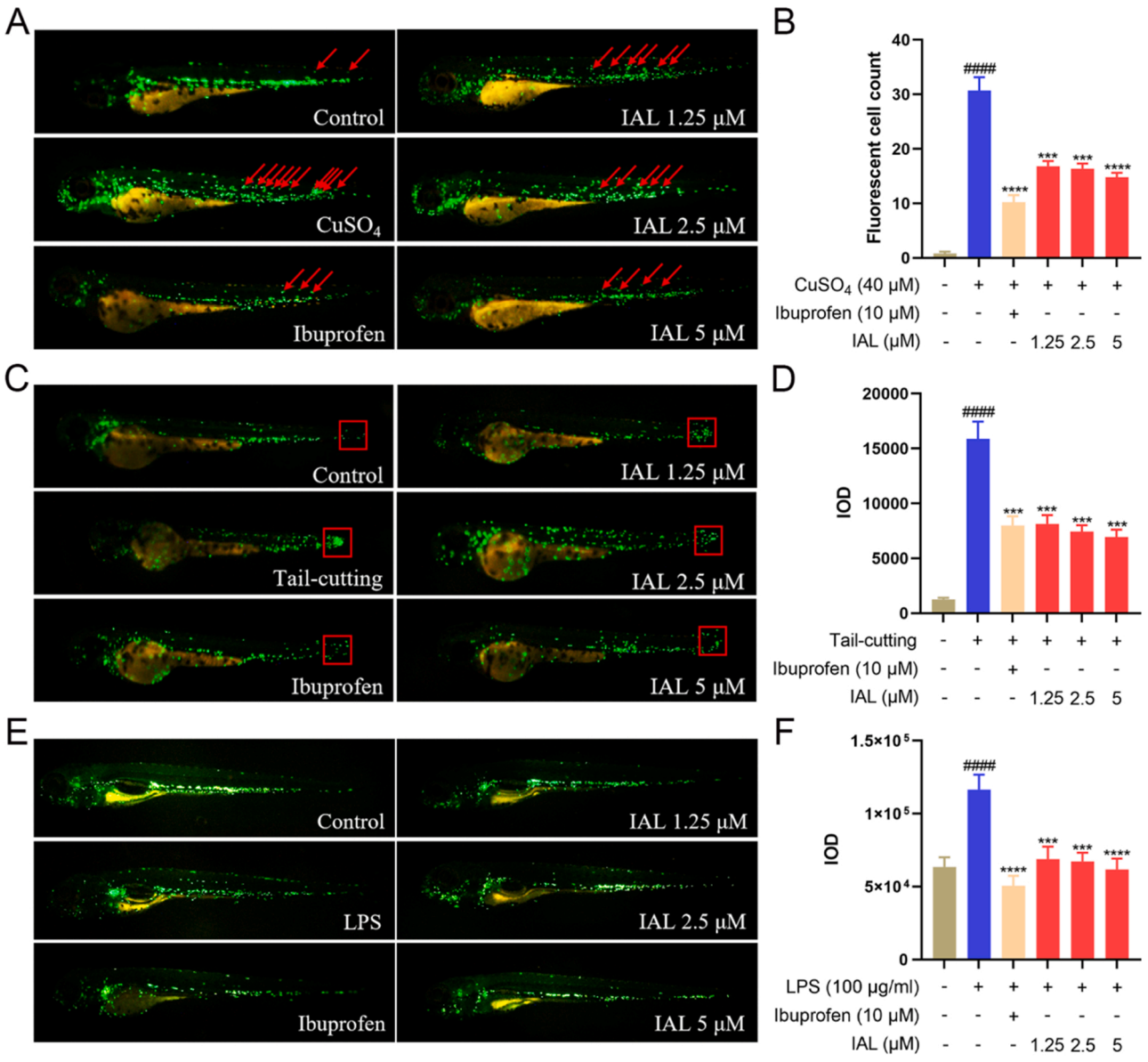

Fig. 3. IAL inhibits $CuSO_4$, tail-cutting, and LPS-induced inflammatory responses in zebrafish. (A) Changes of zebrafish immune cell migration in $CuSO_4$-induced inflammatory model. The red arrows indicate inflammatory cells that migrated to the lateral line. (B) The number of inflammatory cells that migrated to the lateral line. (C) Changes of zebrafish immune cell migration in the tail cutting-induced inflammatory model. The red boxes indicate inflammatory cells that accumulate in the tail. (D) The IOD values of immune cells accumulated in the tail. (E) Changes of zebrafish immune cell migration in the LPS-induced inflammatory model. (F) The IOD values of zebrafish systemic immune cells. Data are expressed as mean ± SEM (n = 10). ####P < 0.0001 vs. the control group, ***P < 0.001, ****P < 0.0001 vs. the model group.

3.5. Network pharmacology analysis

3.5.1. "IAL-targets-GU" network construction

A total of 194 IAL targets and 5115 GU-related targets were obtained by searching various databases. According to Venn analysis, 137 potential targets of IAL against GU were screened (Fig. 5A). The "IAL-targets-GU" visualization network diagram (Fig. 5B) was drawn using Cytoscape v.3.9.0 software. It contains 140 nodes and 973 edges.

3.5.2. PPI network

The PPI network was constructed with 136 nodes and 1072 edges (Fig. 6). The larger the degree value of a node, the larger the node in the graph. Targets with a degree value ≥ 50 include ALB, EGFR, SRC, HSP90AA1, CASP3, ESR1, and MMP9.

3.5.3. Bioinformatic annotation

In the GO enrichment analysis, 78 GO ontology items were screened based on PValue≤ 0.01 and FDR≤ 0.05, of which 42 were related to biological process (BP) and 4 were related to cell component (CC). The other 32 items were related to molecular function (MF). Fig. 7A shows the top 20 GO entries. In BP-related items, the anti-GU effect of IAL was mainly involved in peptidyl-tyrosine phosphorylation, positive regulation of cell proliferation, positive regulation of transcription from RNA polymerase II promoter, positive regulation of MAPK cascade, positive regulation of phosphatidylinositol 3-kinase (PI3K) signaling, *etc*. Whereas in CC-related items, IAL mainly acted on receptor complex. In MF-related items, IAL mainly regulated RNA polymerase II transcription factor activity, protein tyrosine kinase activity, transmembrane receptor protein tyrosine kinase activity, *etc*.

In the KEGG enrichment analysis, 85 signaling pathways were screened based on PValue≤ 0.01 and FDR≤ 0.05, of which the top 20

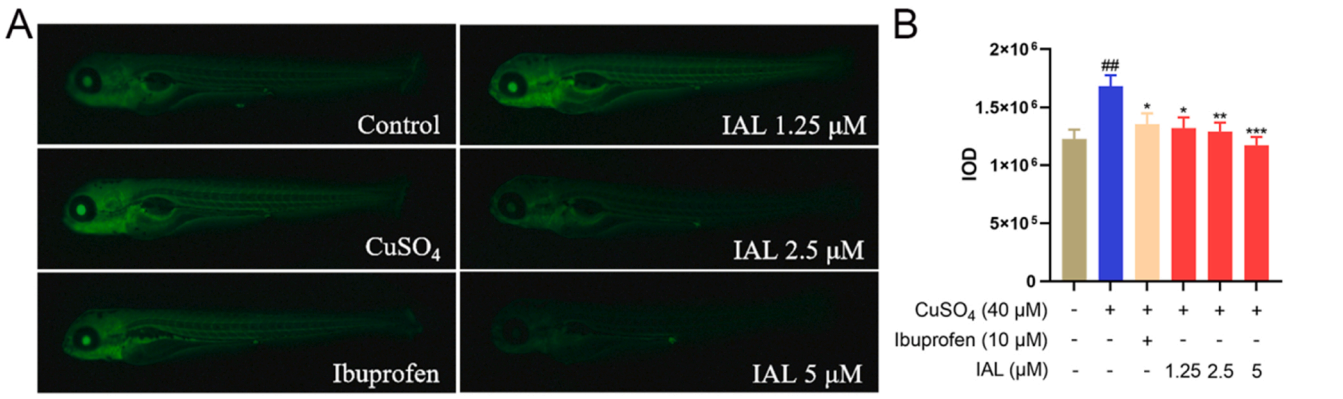

Fig. 4. IAL alleviated inflammation in zebrafish larvae by inhibiting $CuSO_4$-induced ROS production. (A) Microphotographs exhibited ROS production in zebrafish larvae. (B) IAL dose-dependently reduced ROS generation induced by $CuSO_4$. Data are expressed as mean ± SEM (n = 10). ##P < 0.01 vs. the control group, *P < 0.05, **P < 0.01, ***P < 0.001 vs. the model group.

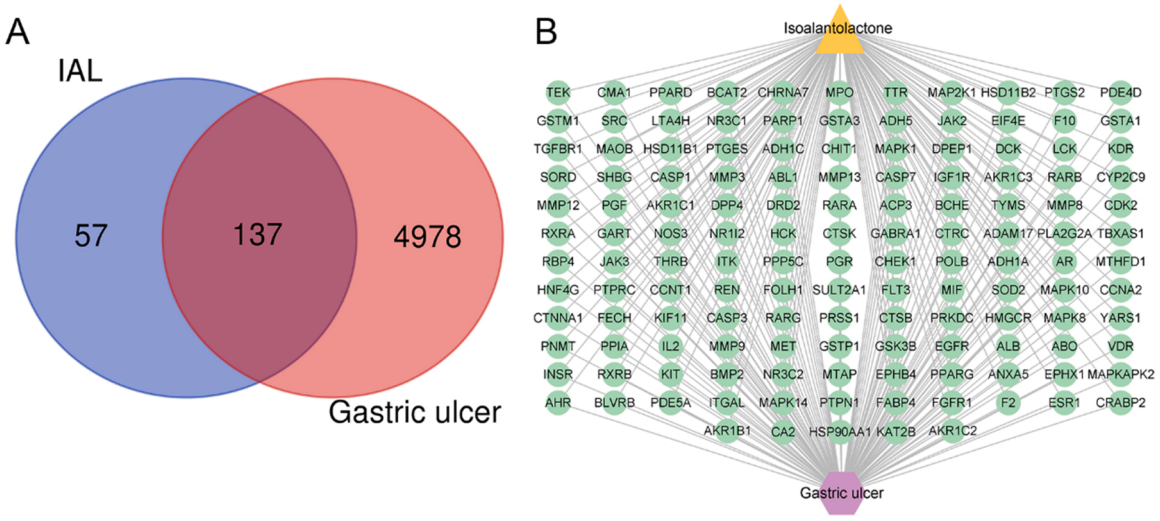

Fig. 5. Venn diagram and "IAL-targets-GU" network diagram. (A) Venn diagram of targets between IAL and GU. (B) The "IAL-targets-GU" visualization network diagram.

were shown in Fig. 7B. The results showed that the potential targets of IAL in anti-GU were involved in many inflammatory and immune-related signaling pathways, such as PI3K-Akt signaling pathway, Th17 cell differentiation, IL-17 signaling pathway, MAPK signaling pathway, and TNF signaling pathway.

3.6. Molecular docking verification of key targets

According to the degree value, the top 5 targets in the PPI network include ALB, EGFR, SRC, HSP90AA1, and CASP3. The binding activity of IAL to these targets was verified by molecular docking, and the obtained LibDock Scores were 82.7461, 62.1062, 80.2834, 86.2359, and 61.2049, respectively (Table 2). The results showed that IAL had a good binding affinity with these tested targets. The molecular docking results were shown in Fig. 8. IAL interacts with amino acid residues of ALB protein through a Carbon Hydrogen bond, Pi-Sigma, Alkyl, and Pi-Alkyl. The main forces between IAL and EGFR include a conventional Hydrogen bond, Alkyl, and Pi-Alkyl. IAL interacts with SRC only through Alkyl, and Pi-Alkyl. The key forces between IAL and HSP90AA1 are conventional Hydrogen bonds, Pi-Sigma, Alkyl, and Pi-Alkyl. IAL interacts with CASP3 through a conventional Hydrogen bond, Carbon Hydrogen bond, Alkyl, and Pi-Alkyl.

3.7. Quantitative real-time PCR

Based on the predicted results of network pharmacology analysis, *mapk14*, *mapk10*, *mapk8*, *mapk1*, *map2k1*, *egfr*, *fgfr1*, *rxra*, *rxrb*, *rara*, and *pgf* genes were enriched in PI3K-Akt signaling pathway and Th17 cell differentiation. Therefore, we verified the effect of IAL on the expression of these genes in a zebrafish model. In addition, we also studied the expression of three inflammatory genes, such as *tnf-α*, *ifn-γ*, and *tgf-β1*. The results showed that IAL treatment down-regulated the expression levels of *mapk14a*, *mapk14b*, *mapk8b*, *mapk1*, *map2k1*, *mapk10*, *egfr*, *fgfr1*, *tnf-α*, and *ifn-γ* in $CuSO_4$-induced inflammatory zebrafish. Whereas, there was significant up-regulation in the expression levels of *rxra*, *rxrb*, *rara*, *pgf*, and *tgf-β1* (Fig. 9).

4. Discussion

Gastric ulcer (GU) is one of the most common digestive diseases characterized by decreased blood flow, neutrophil infiltration, and secretion of inflammatory cytokines [15]. It is well known that GU is closely related to inflammation. Tibetan medicine has a long history in the treatment of digestive diseases. We previously proved that IAL might be a potential effective component of SWG in treating GU. In addition, IAL is one of the common bioactive compounds in Aucklandiae Radix and Inulae Radix that exhibits anti-inflammatory activity [16].

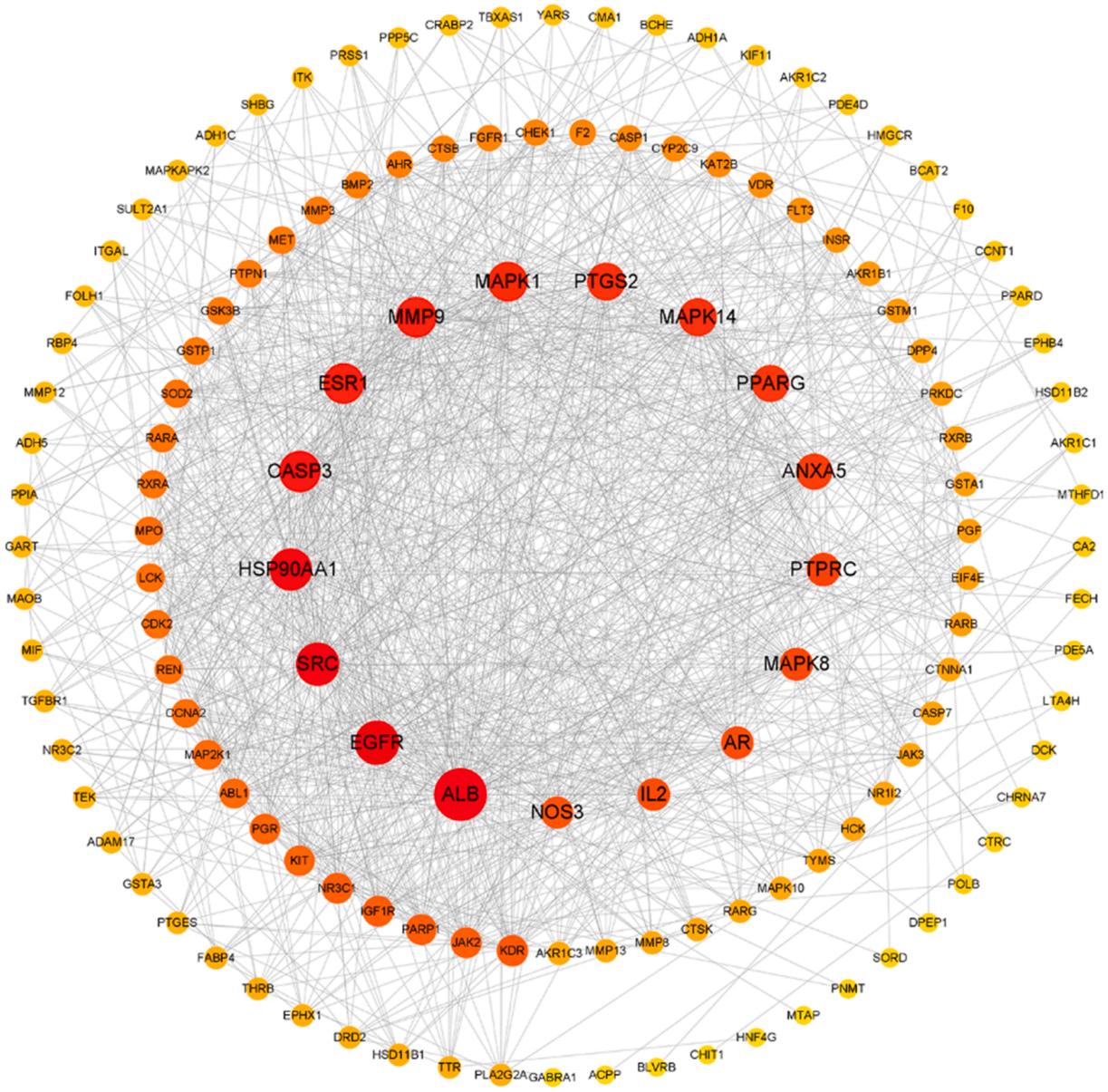

Fig. 6. The "protein-protein interaction" (PPI) network diagram.

Aucklandiae Radix and Inulae Radix have been traditionally used to treat GU. However, the effect of IAL on GU is unclear. This study reports the effect of IAL on GES-1 cells damage, its anti-inflammatory effects in vivo through various inflammation models using zebrafish, explored the potential mechanism of IAL against GU by using network pharmacology and molecular docking studies as well as validation of target gene through qPCR analysis. Based on these results, IAL exhibited showed potential alleviative effects on GU in vitro, *in silico* analysis, and anti-inflammatory effects in vivo zebrafish.

Ethanol is a risk factor for GU [17]. Protecting gastric mucosa is an effective method to treat GU. At present, there are numerous publications that use GES-1 cells and rats to assess the protective effects of traditional Chinese medicine and their extracts, polysaccharides, piperine, and other compounds on ethanol-induced gastric mucosal injury in vitro and in vivo [1], [18], [19]. In this study, the ethanol-induced GES-1 cells injury model was used to evaluate the protective effect of IAL against gastric injury. Ethanol exposure produces an acute inflammatory response that alters the levels of inflammatory cytokines [20]. The results showed that IAL dose-dependently increased the survival rate of ethanol-injured GES-1 cells, as well as IAL at 1.25, 2.5, and 5 μM had no cytotoxicity. Moreover, IAL treatment reduced the levels of pro-inflammatory cytokines TNF-α, IL-1β, and IFN-γ in the cell culture supernatant, while the level of anti-inflammatory cytokine IL-10, TGF-β1, and VEGFA significantly increased compared with the model group, indicating that IAL has a protective effect on ethanol-induced gastric injury. These results verify our hypothesis that IAL is the active component of SWG in treating GU. The anti-GU effect of IAL will be validated in the future using a rat model.

The experimental results of the ethanol-induced GES-1 cell injury model in this study showed that IAL mainly protected gastric mucosal epithelial cells by alleviating inflammation. *In vitro* anti-inflammatory activity of IAL was demonstrated in the literature. It reported that IAL could reduce the production of inflammatory mediators in LPS-stimulated BV2 microglia, peritoneal macrophages, and RAW 264.7 macrophages [10], [21]. However, the anti-inflammatory effect of IAL on animal models is currently unclear. Zebrafish, a complete vertebrate organ system, display inflammatory cells and immune responses similar to humans, while the transparency of zebrafish larvae enables

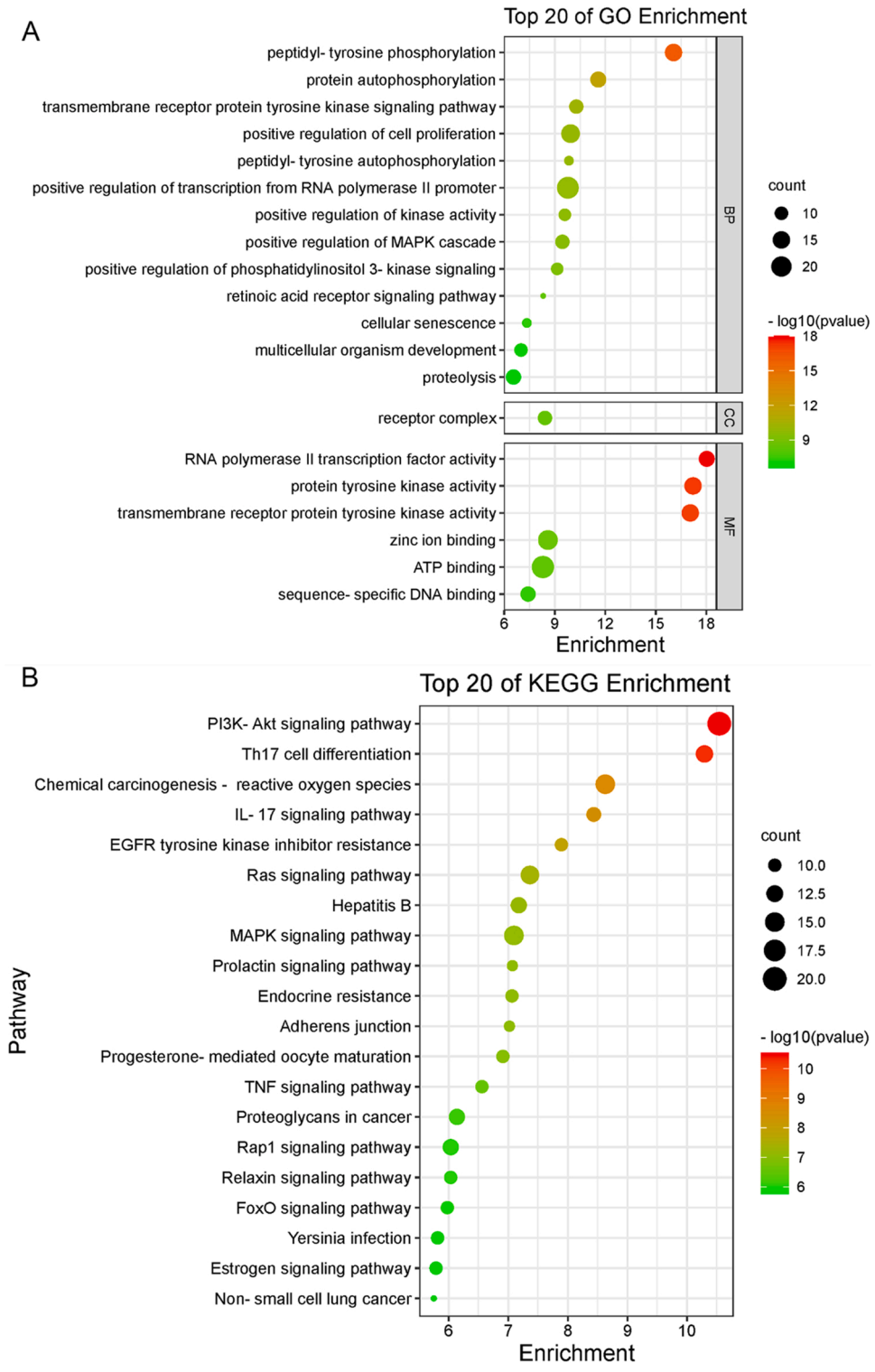

Fig. 7. GO and KEGG enrichment analysis. (A) GO enrichment analysis diagram. (B) KEGG enrichment analysis diagram.

Table 2
The LibDock Scores of 5 core targets and IAL.

Number	Target	Degree	PDB ID	LibDock Score
1	ALB	77	1N5U	82.7461
2	EGFR	58	5UG9	62.1062
3	SRC	56	2H8H	80.2834
4	HSP90AA1	54	6EYA	86.2359
5	CASP3	52	5IBP	61.2049

visualization of inflammatory cell migration. The method of using zebrafish models to study inflammation has been well established. The anti-inflammatory activity of IAL in $CuSO_4$, tail-cutting, and LPS-induced zebrafish inflammation models were studied. In all these models, IAL significantly inhibited the inflammatory response in a dose-dependent manner. Exposure to $CuSO_4$ significantly increases ROS production in zebrafish, and inhibiting this excess ROS generation can effectively impede the progression of the inflammatory response [22]. In this study, IAL reduced the accumulation of ROS in zebrafish cells

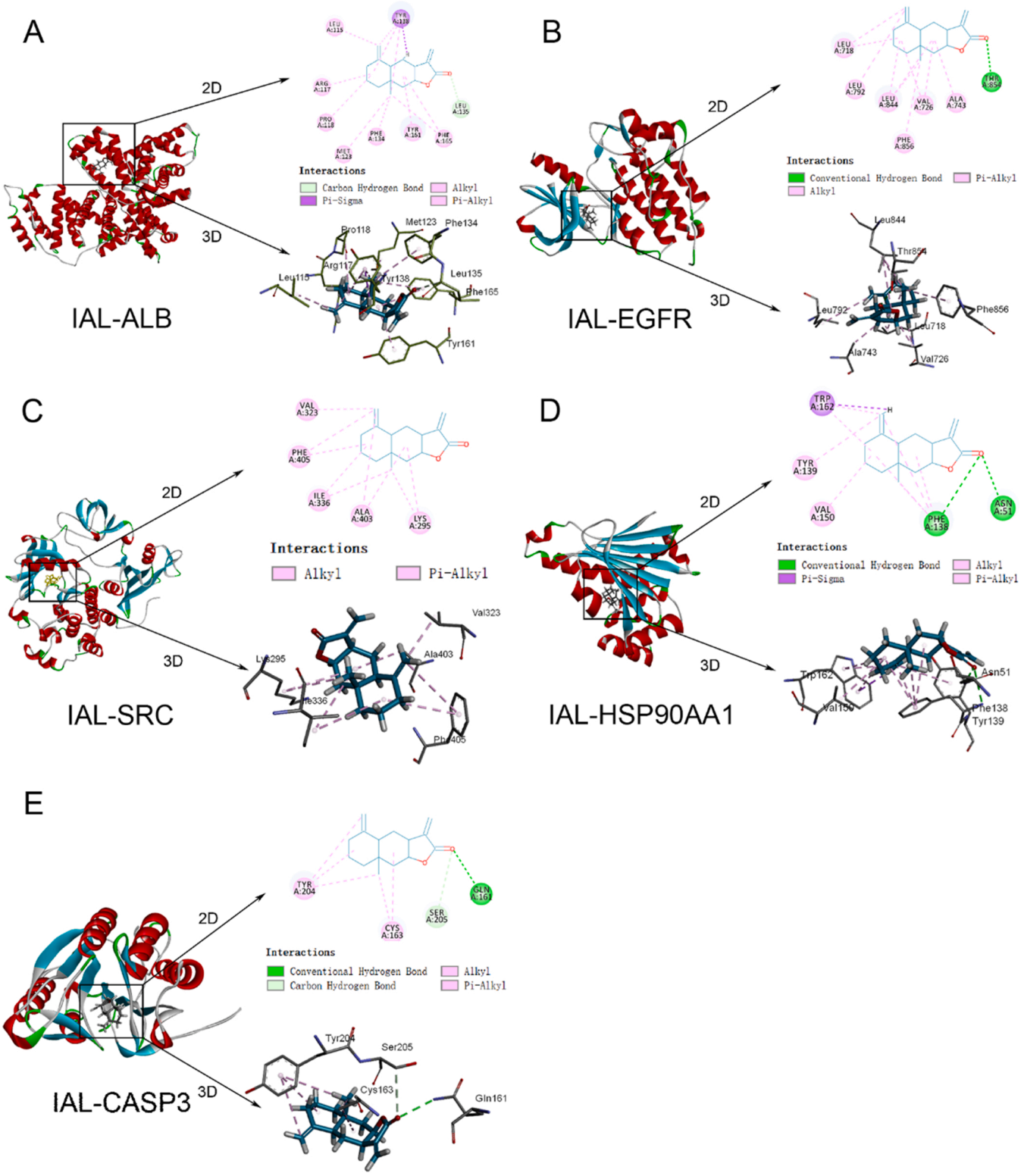

Fig. 8. Molecular docking of IAL with 5 targets protein. Interaction of IAL with the target ALB (A), EGFR (B), SRC (C), HSP90AA1 (D), and CASP3 (E).

induced by $CuSO_4$.

Network pharmacology analysis systematically assesses the effects of drugs on human biological networks [23]. In this study, a total of 137 intersecting targets were screened through network pharmacology analysis, and an "IAL-targets-GU" network was constructed. The PPI network showed that ALB, EGFR, SRC, HSP90AA1, and CASP3 had a high degree value and played an indispensable role in gene regulation. The occurrence of GU causes a decrease in ALB and an increase in other proteins, while serum albumin is used as a predictor of upper gastrointestinal bleeding [24]. EGFR is involved in cell proliferation signaling and is overexpressed in damaged gastric epithelial cells as well as in gastric cancer [25]. The enzymatic activity of SRC is important in the inflammatory response, and it can activate NF-kB and cause gastric inflammation [14]. As a multifunctional molecular chaperone, HSP90

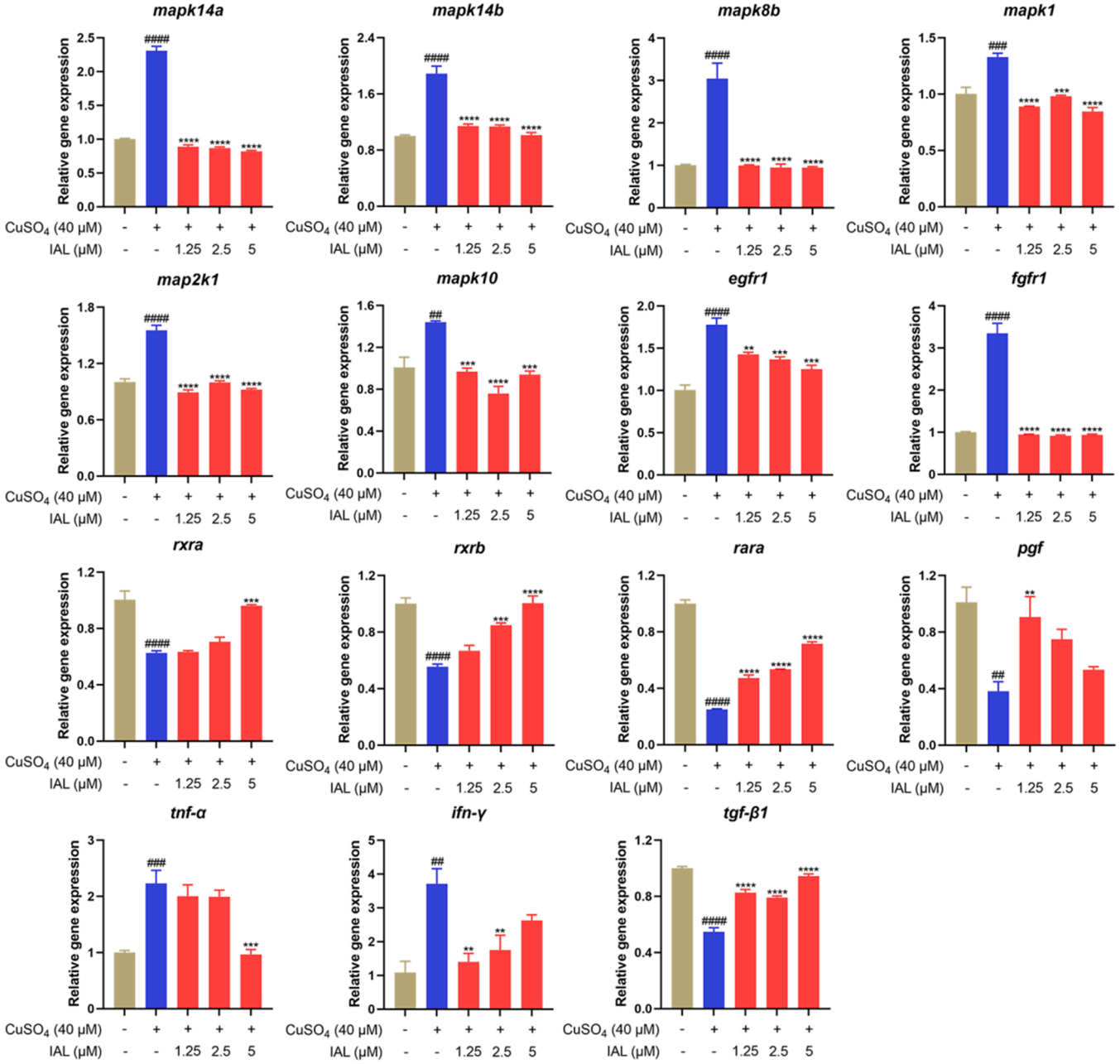

Fig. 9. Effect of IAL on the expression levels of inflammation-related genes in zebrafish. Data are expressed as mean ± SEM (n = 3). ##P < 0.01, ###P < 0.001, ####P < 0.0001 vs. the control group, **P < 0.01, ***P < 0.001, ****P < 0.0001 vs. the model group.

can promote the trafficking, folding, and rearrangement of other proteins, and HSP90 is induced when cells are exposed to inflammation, infection, or ischemia [26]. Further, Caspase-3 (CASP3) is associated with apoptosis during mitochondrial injury and plays an important role in the destruction of gastric mucosal integrity by ethanol exposure [27]. Hence, these targets play a crucial role in cell homeostasis, survival, and proliferation.

In the GO enrichment analysis, potential targets of IAL were involved in multiple inflammation-related biological processes, such as positive regulation of cell proliferation, MAPK cascade, and PI3K signaling. The KEGG enrichment analysis included 85 signaling pathways, and the results showed that the potential targets of IAL in anti-GU were distributed in different signaling pathways, mainly related to inflammation. Among these pathways, PI3K-Akt signaling pathway and Th17 cell differentiation are noteworthy. Activation of the PI3K-Akt signaling pathway is essential for cell proliferation and migration as well as a key factor in ulcer healing and re-epithelialization [28]. Th17 cells contribute to the maintenance of gastrointestinal homeostasis and play an important role in the pathogenesis of various inflammations [29].

Molecular docking is an *in silico* target prediction tool that has been widely used for ligand-based target prediction [30]. Molecular docking results showed that IAL successfully docked with ALB, EGFR, SRC, HSP90AA1, and CASP3, and had a good binding ability, which was verified with the analysis results of network pharmacology.

In addition, the mRNA expression levels of inflammation-related genes enriched in the PI3K-Akt signaling pathway and Th17 cell differentiation were studied by qPCR in zebrafish. Activation of MAPK is crucial for protecting cellular damage and inflammation induced by various toxicants [31]. Studies have shown that Weibing Formula 1 may exert an anti-gastritis effect by inhibiting the expression of EGFR [32]. FGFR1 is a fibroblast growth factor receptor that allows T cells to respond to fibroblast growth factors (FGF) expressed upon injury and

inflammatory responses [33]. Retinoic acid receptors (RARs) are ligand-controlled transcriptional regulators that bind to Retinoid X receptors (RXRs) to regulate cell growth and survival [34]. PGF is homologous to vascular endothelial growth factor (VEGF) and is expressed in anti-inflammatory M2 macrophages [35]. Macrophages typically exist in two distinct subpopulations, the pro-inflammatory M1 macrophages that polarize with Th1 cytokines such as IFN-γ and produce pro-inflammatory cytokines such as TNF-α. Whereas, M2 macrophages have anti-inflammatory and immunomodulatory effects, are polarized by Th2 cytokines, and produce anti-inflammatory cytokines such as TGF-β [36]. In this study, IAL treatment reduced the expression levels of *mapk14a*, *mapk14b*, *mapk8b*, *mapk1*, *map2k1*, *mapk10*, *egfr*, *fgfr1*, *tnf-α*, and *ifn-γ* in $CuSO_4$-induced inflammatory zebrafish. The mRNA expressions of *rxra*, *rxrb*, *rara*, *pgf*, and *tgf-β1* all up-regulated in IAL-treated zebrafish compared with the model group. Hence, IAL showed potential anti-inflammatory effects by regulating various genes responsible for cell survival and inflammation.

5. Conclusion

This study demonstrated the protective effect of IAL against the ethanol-induced injury of GES-1 cells. In addition, the anti-inflammatory effects of IAL were also revealed in zebrafish models. Further, this study is the first to elucidate that ALB, EGFR, SRC, HSP90AA1, and CASP3 are the key targets involved in the network regulation of the IAL anti-GU by using network pharmacology and molecular docking techniques. KEGG enrichment analysis and qPCR analysis results suggest that IAL protects against GU via alleviating inflammation through regulation of PI3K-Akt signaling pathway and Th17 cell differentiation. However, further in-depth studies are necessary to gain more insights and validate the alleviative effect of IAL on gastric injuries.

Funding

This work was supported by the Tibet Autonomous Region Science and Technology Planning Project (XZ202201YD0009C); Shandong Provincial Natural Science Foundation (ZR2020YQ60, ZR2021QH155); Shandong Provincial Central Guidance Local Science and Technology Development Fund Project (YDZX2022164, YDZX2021023); and Jinan Talent Project for University (2021GXRC047, 2020GXRC053).

CRediT authorship contribution statement

Chaoyi Zhou: Investigation, Formal analysis, Data curation, Writing – original draft. **Jing Chen:** Validation, Formal analysis, Writing – review & editing. **Kechun Liu:** Methodology, Supervision. **Kannan Maharajan:** Formal analysis, Writing – original draft, Writing – review & editing. **Yun Zhang:** Methodology, Writing – review & editing. **Linhua Hou:** Validation, Data curation, Writing – original draft. **Jianheng Li:** Conceptualization, Methodology, Formal analysis, Writing – review & editing, Visualization, Project administration. **Ma Mi:** Conceptualization, Methodology, Formal analysis, Writing – review & editing, Visualization, Project administration. **Qing Xia:** Conceptualization, Methodology, Formal analysis, Writing - original draft, Writing – review & editing, Visualization, Project administration, Funding acquisition.

Conflict of Interest statement

The authors declare that there are no conflicts of interest.

Conflict of interest statement

The authors declare that they have no known competing financial interests or personal relationships that could have appeared to influence the work reported in this paper.

References

[1] S. Fu, J. Chen, C. Zhang, J. Shi, X. Nie, Y. Hu, C. Fu, X. Li, J. Zhang, Gastroprotective effects of Periplaneta americana L. extract against ethanol-induced gastric ulcer in mice by suppressing apoptosis-related pathways, Front. Pharmacol. 12 (2021), 798421.
[2] M.S. Shin, J. Lee, J.W. Lee, S.H. Park, I.K. Lee, J.A. Choi, J.S. Lee, K.S. Kang, Anti-inflammatory effect of Artemisia argyi on ethanol-induced gastric ulcer: analytical, in vitro and in vivo studies for the identification of action mechanism and active compounds, Plants (Basel) 10 (2) (2021) 332.
[3] M. Li, R. Lv, X. Xu, Q. Ge, S. Lin, Tricholoma matsutake-derived peptides show gastroprotective effects against ethanol-induced acute gastric injury, J. Agric. Food Chem. 69 (49) (2021) 14985–14994.
[4] X. Liu, S. Quan, Q. Han, J. Li, X. Gao, J. Zhang, D. Liu, Effectiveness of the fruit of Rosa odorata sweet var. gigantea (Coll. et Hemsl.) Rehd. et Wils in the protection and the healing of ethanol-induced rat gastric mucosa ulcer based on Nrf2/NF-κB pathway regulation, J. Ethnopharmacol. 282 (2022), 114626.
[5] Y. Zhang, J. Liang, H. Jiang, M. Qian, W. Zhao, W. Bai, Protective effect of sterols extracted from Lotus plumule on ethanol-induced injury in GES-1 cells in vitro, Food Funct. 12 (24) (2021) 12659–12670.
[6] R. Xu, Y. Peng, M. Wang, X. Li, Intestinal absorption of isoalantolactone and alantolactone, two sesquiterpene lactones from Radix Inulae, using Caco-2 cells, Eur. J. Drug Metab. Pharmacokinet. 44 (2) (2019) 295–303.
[7] J. Lu, Z. Kuang, T. Chen, C. Ye, W. Hou, L. Tang, Y. Chen, R. He, Isoalantolactone inhibits RANKL-induced osteoclast formation via multiple signaling pathways, Int. Immunopharmacol. 84 (2020), 106550.
[8] Y. Song, X. Li, F. Liu, H. Zhu, Y. Shen, Isoalantolactone alleviates ovalbumin-induced asthmatic inflammation by reducing alternatively activated macrophage and STAT6/PPAR-γ/KLF4 signals, Mol. Med. Rep. 24 (4) (2021) 701.
[9] Y.H. Ding, Y.D. Song, Y.X. Wu, H.Q. He, T.H. Yu, Y.D. Hu, D.P. Zhang, H.C. Jiang, K.K. Yu, X.Z. Li, L. Sun, F. Qian, Isoalantolactone suppresses LPS-induced inflammation by inhibiting TRAF6 ubiquitination and alleviates acute lung injury, Acta Pharmacol. Sin. 40 (1) (2019) 64–74.
[10] G. He, X. Zhang, Y. Chen, J. Chen, L. Li, Y. Xie, Isoalantolactone inhibits LPS-induced inflammation via NF-κB inactivation in peritoneal macrophages and improves survival in sepsis, Biomed. Pharmacother. 90 (2017) 598–607.
[11] C.A. MacRae, R.T. Peterson, Zebrafish as tools for drug discovery, Nat. Rev. Drug Discov. 14 (10) (2015) 721–731.
[12] M.A.A. Belo, M.F. Oliveira, S.L. Oliveira, M.F. Aracati, L.F. Rodrigues, C.C. Costa, G. Conde, J.M.M. Gomes, M.N.L. Prata, A. Barra, T.M. Valverde, D.C. de Melo, S. F. Eto, D.C. Fernandes, M. Romero, J.D. Correa Junior, J.O. Silva, A.L.B. Barros, A. C. Perez, I. Charlie-Silva, Zebrafish as a model to study inflammation: a tool for drug discovery, Biomed. Pharmacother. 144 (2021), 112310.
[13] R. Zanandrea, C.D. Bonan, M.M. Campos, Zebrafish as a model for inflammation and drug discovery, Drug Discov. Today 25 (12) (2020) 2201–2211.
[14] S. Ren, Y. Wei, M. Niu, R. Li, R. Wang, S. Wei, J. Wen, D. Wang, T. Yang, X. Chen, S. Wu, Y. Tong, M. Jing, H. Li, M. Wang, Y. Zhao, Mechanism of rutaecarpine on ethanol-induced acute gastric ulcer using integrated metabolomics and network pharmacology, Biomed. Pharmacother. 138 (2021), 111490.
[15] Z. Zhao, S. Gong, S. Wang, C. Ma, Effect and mechanism of evodiamine against ethanol-induced gastric ulcer in mice by suppressing Rho/NF-κB pathway, Int. Immunopharmacol. 28 (1) (2015) 588–595.
[16] K. Zhuang, Q. Xia, S. Zhang, K. Maharajan, K. Liu, Y. Zhang, A comprehensive chemical and pharmacological review of three confusable Chinese herbal medicine-Aucklandiae radix, Vladimiriae radix, and Inulae radix, Phytother. Res. 35 (12) (2021) 6655–6689.
[17] R.O. Formiga, E.B. Alves Junior, R.C. Vasconcelos, A.A. Araujo, T.G. de Carvalho, R.F. de Araujo Junior, G.B.C. Guerra, G.C. Vieira, K.M. de Oliveira, M. Diniz, M. V. Sobral, J.M. Barbosa Filho, F. Spiller, L.M. Batista, Effect of p-cymene and rosmarinic acid on gastric ulcer healing - involvement of multiple endogenous curative mechanisms, Phytomedicine 86 (2021), 153497.
[18] C. Hou, L. Liu, J. Ren, M. Huang, E. Yuan, Structural characterization of two Hericium erinaceus polysaccharides and their protective effects on the alcohol-induced gastric mucosal injury, Food Chem. 375 (2022), 131896.
[19] Z. Duan, S. Yu, S. Wang, H. Deng, L. Guo, H. Yang, H. Xie, Protective effects of piperine on ethanol-induced gastric mucosa injury by oxidative stress inhibition, Nutrients 14 (22) (2022) 4744.
[20] L. Xie, Y.L. Guo, Y.R. Chen, L.Y. Zhang, Z.C. Wang, T. Zhang, B. Wang, A potential drug combination of omeprazole and patchouli alcohol significantly normalizes oxidative stress and inflammatory responses against gastric ulcer in ethanol-induced rat model, Int. Immunopharmacol. 85 (2020), 106660.
[21] M. Wang, K. Wang, X. Gao, K. Zhao, H. Chen, M. Xu, Anti-inflammatory effects of isoalantolactone on LPS-stimulated BV2 microglia cells through activating GSK-3β-Nrf2 signaling pathway, Int. Immunopharmacol. 65 (2018) 323–327.
[22] L. Gong, L. Yu, X. Gong, C. Wang, N. Hu, X. Dai, C. Peng, Y. Li, Exploration of anti-inflammatory mechanism of forsythiaside A and forsythiaside B in $CuSO_4$-induced inflammation in zebrafish by metabolomic and proteomic analyses, J. Neuroinflamm. 17 (1) (2020) 173.
[23] C. Li, R. Wen, D. Liu, L. Yan, Q. Gong, H. Yu, Assessment of the potential of Sarcandra glabra (Thunb.) Nakai. in treating ethanol-induced gastric ulcer in rats based on metabolomics and network analysis, Front. Pharmacol. 13 (2022), 810344.
[24] M. Koushki, R. Farrokhi Yekta, N. Amiri-Dashatan, M. Dadpay, F. Goshadrou, Therapeutic effects of hydro-alcoholic extract of Achillea wilhelmsii C. Koch on indomethacin-induced gastric ulcer in rats: a proteomic and metabolomic approach, BMC Complement. Altern. Med. 19 (1) (2019) 205.

[25] S. George, Y. Lucero, J.P. Torres, A.J. Lagomarcino, M. O'Ryan, Gastric damage and cancer-associated biomarkers in helicobacter pylori-infected children, Front. Microbiol. 11 (2020) 90.
[26] H. Guo, B. Chen, Z. Yan, J. Gao, J. Tang, C. Zhou, Metabolites profiling and pharmacokinetics of troxipide and its pharmacodynamics in rats with gastric ulcer, Sci. Rep. 10 (1) (2020) 13619.
[27] D. Zhou, Q. Yang, T. Tian, Y. Chang, Y. Li, L.R. Duan, H. Li, S.W. Wang, Gastroprotective effect of gallic acid against ethanol-induced gastric ulcer in rats: Involvement of the Nrf2/HO-1 signaling and anti-apoptosis role, Biomed. Pharmacother. 126 (2020), 110075.
[28] H.H. Arab, S.A. Salama, A.H. Eid, A.M. Kabel, N.N. Shahin, Targeting MAPKs, NF-kappaB, and PI3K/AKT pathways by methyl palmitate ameliorates ethanol-induced gastric mucosal injury in rats, J. Cell. Physiol. 234 (12) (2019) 22424–22438.
[29] N. Garrido-Mesa, F. Algieri, A. Rodriguez Nogales, J. Galvez, Functional plasticity of Th17 cells: Implications in gastrointestinal tract function, Int. Rev. Immunol., 32 ((5–6) (2013) 493–510.
[30] Y. Wang, Y.W. Sun, Y.M. Wang, Y. Ju, D.L. Meng, Virtual screening of active compounds from Artemisia argyi and potential targets against gastric ulcer based on network pharmacology, Bioorg. Chem. 88 (2019), 102924.
[31] X. Chang, F. Luo, W. Jiang, L. Zhu, J. Gao, H. He, T. Wei, S. Gong, T. Yan, Protective activity of salidroside against ethanol-induced gastric ulcer via the MAPK/NF-κB pathway in vivo and in vitro, Int. Immunopharmacol. 28 (1) (2015) 604–615.
[32] K. Chen, L. Zhang, Z. Qu, F. Wan, J. Li, Y. Yang, H. Yan, S. Huang, Uncovering the mechanisms and molecular targets of Weibing Formula 1 against gastritis: Coupling network pharmacology with GEO database, Biomed. Res. Int. 2021 (2021) 5533946.
[33] B. Chen, C. Li, G. Chang, H. Wang, Dihydroartemisinin targets fibroblast growth factor receptor 1 (FGFR1) to inhibit interleukin 17A (IL-17A)-induced hyperproliferation and inflammation of keratinocytes, Bioengineered 13 (1) (2022) 1530–1540.
[34] L. Altucci, M.D. Leibowitz, K.M. Ogilvie, A.R. de Lera, H. Gronemeyer, RAR and RXR modulation in cancer and metabolic disease, Nat. Rev. Drug Discov. 6 (10) (2007) 793–810.
[35] N. Jetten, S. Verbruggen, M.J. Gijbels, M.J. Post, M.P. De Winther, M.M. Donners, Anti-inflammatory M2, but not pro-inflammatory M1 macrophages promote angiogenesis in vivo, Angiogenesis 17 (1) (2014) 109–118.
[36] A. Shapouri-Moghaddam, S. Mohammadian, H. Vazini, M. Taghadosi, S. A. Esmaeili, F. Mardani, B. Seifi, A. Mohammadi, J.T. Afshari, A. Sahebkar, Macrophage plasticity, polarization, and function in health and disease, J. Cell. Physiol. 233 (9) (2018) 6425–6440.